



Effects of hydrogen in working gas for sputter-deposition on surface morphology and microstructure of indium tin oxide thin films grown at room temperature

著者	Luo Suning, Kohiki Shigemi, Okada Koichi, Mitome Masanori, Shoji Fumiya
journal or publication title	Materials Letters
volume	63
number	27
page range	2365-2368
year	2009-11-15
その他のタイトル	
URL	http://hdl.handle.net/10228/00006432

doi: [info:doi/10.1016/j.matlet.2009.08.010](https://doi.org/10.1016/j.matlet.2009.08.010)

Effects of hydrogen in working gas for sputter-deposition on surface morphology and microstructure of indium tin oxide thin films grown at room temperature

Suning Luo,^{a,b} Shigemi Kohiki,^{a,*} Koichi Okada,^a Masanori Mitome,^c and Fumiya Shoji^d

^a*Department of Materials Science, Kyushu Institute of Technology, Kitakyushu 804-8550, Japan*

^b*Liaoning Institute of Technology, China*

^c*National Institute for Materials Science, Tsukuba 305-0044, Japan*

^d*Kyushu Kyoritsu University, Kitakyushu 807-8585, Japan*

ABSTRACT

Surface morphology and microstructure of indium tin oxide (ITO) thin films sputter deposited without heat treatment were obviously different from each other depending on the hydrogen concentration [H] in the working gas. The film surface became smoother with increasing [H] to 1 %, but nucleation and growth of grains were apparent above [H] = 1.5 %. The width of columnar grains in the ≤ 200 nm-thick films narrowed from ≈ 100 nm to ≈ 50 nm with increasing [H] from 0 % to 1.5 %. Randomly oriented and agglomerated grains were observed for the film deposited with [H] = 3.6 %. Hydrogen added to the working gas induced reduction of the grain size, and then resulted in lowering of the carrier mobility.

*Corresponding author. Tel.: +81-93-884-3300; Fax: +81-93-884-3310, E-mail address: kohiki@che.kyutech.ac.jp

1. Introduction

For realizing next-generation optoelectronic devices, thin films of transparent conducting oxides are requested to be far more conductive, while preserving the optical transparency [1-3]. Indium tin oxide (ITO) has been the most widely used transparent conducting oxide in semiconductor and electronic device industry [4-6]. Substitution of In^{3+} ions by Sn^{4+} ions results in not only an increase of the carrier density N but also a decrease of the carrier mobility μ . From the viewpoint of charge neutrality, one oxygen defect generates two n -type carriers in the crystal. Generation of oxygen deficiency in the crystal is an attractive way to achieve both higher conductivity and optical transparency. However, proper selection of the thin film deposition parameters is important to achieve higher conductivity since too many oxygen vacancies in the lattice will turn the crystal into non-stoichiometric, and then too much structural disorder in the lattice will decrease μ and enlarge resistivity of the films.

Thin films of ITO are known to demonstrate a diversity of the electronic properties, surface morphology and microstructure depending on the deposition conditions [7-9]. Higher conductivity and transparency without heat treatment even both in and after the deposition are indispensable for next-generation ITO films applicable to optoelectronic devices using organic-polymer substrates. In our previous paper on the optical and electrical properties of ITO films sputter-deposited in the working gas containing hydrogen without heat treatment, we reported that hydrogen of 1 % in the gas generated oxygen defects leading the largest N , while preserving μ from decay, and resulted in the highest conductivity and transparency [10].

In this work, we examined effects of hydrogen in the working gas on surface morphology and microstructure of the films in relation to their optical and electrical properties. We eliminated heat treatments such as the substrate heating and the post-deposition heating in air to scrutinize thin film growth under irradiation of hydrogen related reducing species. The smoothest and featureless surface was observed for the film deposited in the gas containing hydrogen of 1 % by scanning electron microscopy. Transmission electron microscopy demonstrated that the width of columnar grains in a body from the bottom to the top of the ≈ 200 nm thick film was $\approx 50 - 100$ nm, and the grains oriented basically normal to the substrate surface. The grains still preserved their crystal structure even at interface to the substrate.

2. Experimental

Films of ITO were deposited on glass substrates without substrate heating by *dc* sputtering

of a sintered target (Kojundo Chemical, Japan) in the working gas containing hydrogen. The target consisted of In_2O_3 (95 wt.%) and SnO_2 (5 wt.%). The excitation conditions of columnar plasma for sputter-deposition were as follows: gas pressure of $\approx 1 \times 10^{-3}$ Torr, anode voltage of 75 V, and an anode current of 0.8 A. Deuterium gas (99.99 % purity) and argon gas (99.9999 % purity) were introduced to deposition chamber of the base pressure $\approx 1 \times 10^{-7}$ Torr. Films were deposited at the hydrogen partial pressures of $\approx 1 \times 10^{-7} - 3.6 \times 10^{-5}$ Torr. The gas pressure ratio of hydrogen to argon, denoted as the hydrogen concentration [H] in the deposition, was in the range 0 – 3.6 %.

Surface morphology was examined by a JEOL JSM-6360 scanning electron microscope (SEM) operated at the electron acceleration voltage of 15 kV. Microstructure of cross-sectioned specimens was examined by a JEOL JEM-3100FEF transmission electron microscope (TEM) operated at the electron acceleration voltage of 300 kV. Energy dispersive x-ray spectrometer (EDS) attached on the TEM was also used for elemental analysis.

3. Results and discussion

Figures 1 (a) - (e) demonstrate changes in surface morphology of the films with [H] by SEM. We observed surface corrugation for the film [H] = 0 %. As shown by the Figs. 1 (a) - (c), addition of hydrogen smoothed out such corrugation. The film [H] = 1 % exhibited the smoothest and featureless surface. Further addition of hydrogen up to [H] = 1.5 % resulted in formation of spherical grains with diameter $\Phi \approx 50 - 150$ nm. The featureless surface was studded with the grains, as seen in Fig. 1 (d). Much more addition of hydrogen to [H] = 3.6 % enhanced grain growth ($\Phi < 100 \sim 200$ nm) and agglomeration of the densely populated grains, as depicted by the Fig. 1 (e). We have reported optical transmittance of > 80 % and < 40 % in the wavelength of 400 – 800 nm for the films of [H] < 1.5 % and [H] = 3.6 %, respectively [10]. Observed grain growth and agglomeration on the smooth surface corresponded to the tendency of optical transmittance of the films.

Figures 2 (a) - (d) demonstrate changes in microstructure of the films with [H] by TEM. Thickness of the films with [H] = 0, 1, and 1.5 % were $\approx 150 - 200$ nm. The film [H] = 3.6 %

showed an agglomeration of the grains with $\Phi < 100 \sim 200$ nm. Surface corrugation of the films with $[H] = 0, 1,$ and 1.5 % amounted to ≤ 10 nm, however the surface of the film $[H] = 1$ % looks to be the smoothest. The films with $[H] = 0, 1,$ and 1.5 % demonstrated columnar grains in a body from the bottom to the top. The width of the column in the films with $[H] = 0, 1,$ and 1.5 % were $\approx 100, \approx 50 - 100,$ and $\approx 35 - 70$ nm, respectively. The increase of $[H]$ brought about narrowing of the width of the columnar grains. The grains in the films with $[H] = 0, 1,$ and 1.5 % oriented basically normal to the substrate surface but canted slightly. The interface between the film and the substrate was sharp; neither intermediate phase nor amorphous phase was observed. The absence of amorphous phase at the film-substrate interface indicates that our selection of the deposition conditions achieving the low deposition rate of ≤ 0.03 nm/s was appropriate to obtain high quality as-deposited films without intentional substrate heating.

Despite the progress in grain-size reduction with an increase of $[H]$, high resolution (HR) TEM image of the films with $[H] = 0$ and 1 % indicate that the grains still preserve their single-crystalline structure, as shown in Figs. 3 (a) and (b). On the other hand, the HRTEM images shown in Figs. 3 (c) and (d) revealed that the grains in the films of $[H] = 1.5$ and 3.6 % are obviously poly-crystal with large-angle boundary (41°) and with random orientation, respectively.

Figures 4 (a) and (d) demonstrate the dark field image by scanning TEM of the films with $[H] = 1.5$ and 3.6 %, respectively. As shown in Figs. 4 (b) and (c), the elemental distribution of indium by EDS was coincident with that of oxygen for the film $[H] = 1.5$ %. In the film $[H] = 3.6$ %, the distribution of indium was apparently different from that of oxygen, as shown in Figs. 4 (e) and (f). Especially the distribution of oxygen is not uniform, as depicted by Fig. 4 (f). The regions with size of $\approx 30 - 60$ nm, where indium is rich but oxygen is absent, are seen as the places accompanied with the brightest In L -signal in Fig. 4 (e) and the darkest O K -signal in Fig. 4 (f). Such inconsistency in the elemental distribution suggests reduction of the ITO films by the active species such as hydrogen radicals and ions decomposed in the plasma [11]. Hydrogen radical is a strong reducing species, and liberates oxygen from ITO [12]. The reduction brings about generation of the oxygen defects and n -type carriers [13,14]. Although dissociation of the In–O bond was enhanced in the film $[H] = 3.6$ %, the reported N values were $\approx 4 - 7 \times 10^{20} \text{ cm}^{-3}$ for the films with $[H] = 0 - 3.6$ % [10]. Therefore, we consider the

effect of hydrogen on μ to elucidate the variation of resistivity with [H]. When we assume that a high μ for the films correlates to the single-crystalline structure of the grains, the polycrystalline structure of the grains lowers μ and gives rise to higher resistivity. The reported μ were ≈ 55 , ≈ 30 , and ≈ 10 cm/Vs for the films with [H] < 1 %, $= 1.5$ %, and 3.6 %, respectively [10]. Thus, TEM revealed that an increase in [H] brings about reduction of the grain size, which lowers μ of the films.

4. Summary

SEM and TEM for the ITO films presented the effects of hydrogen addition. The gas composition definitely affected film morphology with relatively smooth films changing to agglomerated spherical grains on the substrate surface with an increase in [H]. The increase of [H] reduced the grain size and changed the grains from single-crystalline structure to polycrystalline structure. The inconsistent distribution of indium and oxygen by EDS indicated that added hydrogen led to reduction of ITO. High resistivity reported for the films [H] ≥ 1.5 % can be related to the reduction in grain size with increasing [H].

Acknowledgement. This work was partly supported by the "Nanotechnology Network Project" of the Ministry of Education, Culture, Sports, Science and Technology, Japan.

References

- [1] D. Ginley, C. Bright, *MRS Bulletin* **25**, 15 (2000).
- [2] C. G. Granqvist, A. Hultaker, *Thin Solid Films* **411**, 1 (2002).
- [3] S. Lany, A. Zunger, *Phys. Rev. Lett.* **98**, 045501 (2007).
- [4] A. Salehi, *Thin Solid Films* **324**, 214 (1998).
- [5] J. K. Sheu, Y. K. Su, G. C. Chi, M. J. Jou, C. M. Chang, *Appl. Phys. Lett.* **72**, 3317 (1998).
- [6] B. Lewis, D. Paine, *MRS Bulletin* **25**, 22 (2000).
- [7] H. Y. Chen, C. F. Qiu, M. Wong, H. S. Kwok, *IEEE Electron Device Lett.* **24**, 315 (2003).
- [8] K. Zhang, F. Zhu, C. H. A. Huan, A. T. Wee, *J. Appl. Phys.* **86**, 974 (1999).
- [9] R. X. Wang, D. Beling, A. B. Djuriscic, S. Li, S. Fung, *Semicond. Sci. Technol.* **19**, 695 (2004).
- [10] S. Luo, K. Okada, S. Kohiki, F. Tsutsui, H. Shimooka, F. Shoji, *Materials Letters* **63**, 641 (2009).
- [11] J. Wallinga, W. M. A. Bik, A. M. Vredenberg, R. E. I. Schropp, W. F. van der Weg, *J. Phys. Chem. B* **102**, 6219 (1998).
- [12] R. Banerjee, S. Ray, N. Basu, A. K. Batabyal, A. K. Barua, *J. Appl. Phys.* **62**, 912 (1987).
- [13] J. H. W. Dewit, *J. Solid State Chem.* **8**, 142 (1973).
- [14] J. H. W. Dewit, G. Vanunen, M. Lahey, *J. Phys. Chem. Solids* **38**, 819 (1977).

Figure captions

Fig. 1 SEM images of the films with [H] = 0 (a), 0.3 (b), 1 (c), 1.5 (d), and 3.6 % (e).

Fig. 2 TEM images of the films with [H] = 0 (a), 1 (b), 1.5 (c), and 3.6 % (d).

Fig. 3 HRTEM images of the films with [H] = 0 (a), 1 (b), 1.5 (c), and 3.6 % (d).

The spacing and the Miller index of corresponding plane are shown in each figure.

Fig. 4 Left panels: dark field image (a) by scanning TEM and elemental maps for indium (b) and oxygen (c) by EDS for the film with [H] = 1.5 %. Right panels: dark field image (d) and elemental maps for indium (e) and oxygen (f) for the film with [H] = 3.6 %. For the film of [H] = 3.6 %, ratios of indium to oxygen in wt.% estimated by EDS varied from 92 : 8 to 100 : 0 depending on the probed position.

Fig. 1

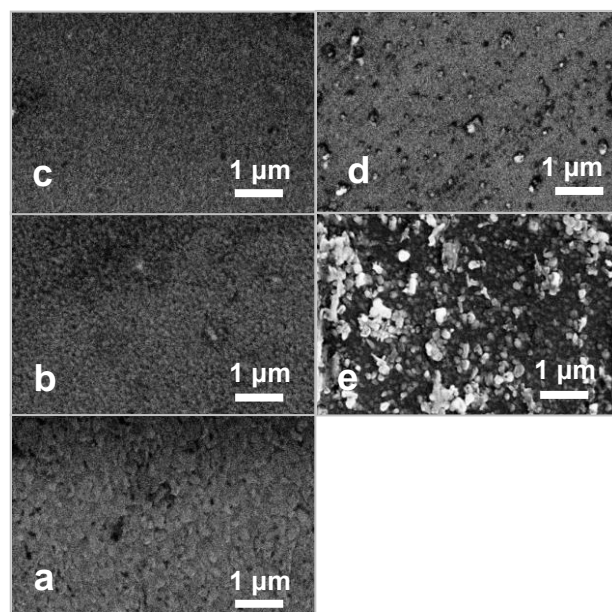


Fig. 2

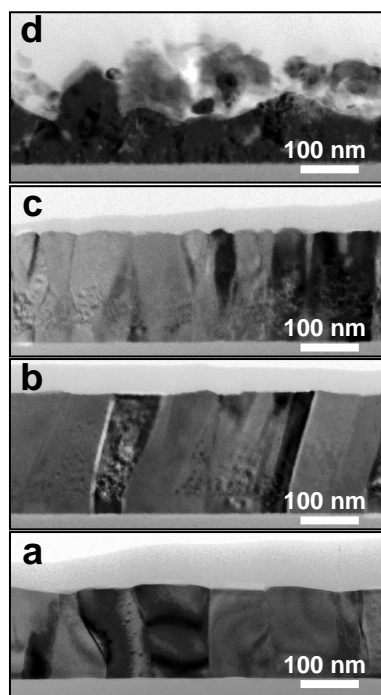


Fig. 3

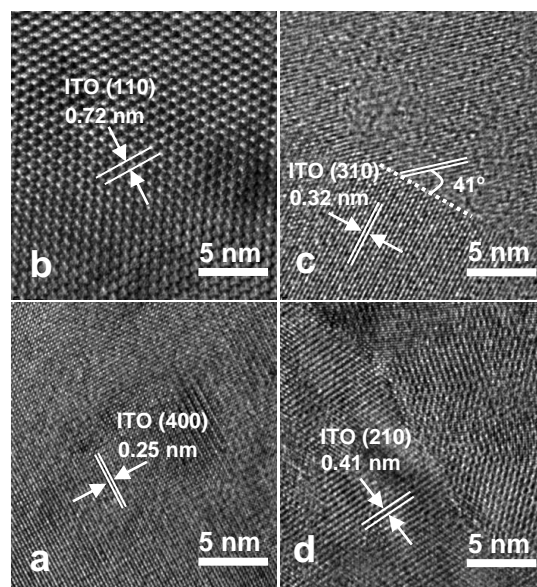


Fig. 4

